

# EMITTANCE MEASUREMENTS OF NANOBLADE-ENHANCED HIGH FIELD CATHODE

G. E. Lawler\*, N. Montanez, J. Mann, N. Majernik, J.B. Rosenzweig,  
UCLA, Los Angeles, California, USA  
V. Yu, RadiaBeam Technologies, Santa Monica, California, USA

## Abstract

High brightness cathodes are increasingly a focus for accelerator applications ranging from free electron lasers to ultrafast electron diffraction. There is further an increasing interest in fabrication and control of cathode surface to better control the emission characteristics and improve beam brightness. One method which we can consider is based on well-known silicon nanofabrication techniques which we use to create patterned cathode surfaces. The sharp edges produced lead to field emission increases and high brightness emission. We have demonstrated that a beam can be successfully extracted with a low emittance and we have reconstructed a portion of the energy spectrum. Due to the simplicity of extended geometries in nanofabrication our beam uniquely possesses a high aspect ratio in its transverse cross section. We can begin to consider modifications for emittance exchange beamlines and having shown the patterning principle is sound we can consider additional patterns such as hollow beams. Future work will continue to characterize the produced beam and the addition of fabrication steps to remove one of the blades in the double blade geometry in order to more accurately characterize the emission.

## INTRODUCTION

The National Science Foundation Center for Bright Beams is currently exploring the limits of electron beam brightness for many applications including free electron lasers, ultrafast electron diffraction, etc. One route is to increase initial brightness at the cathode through nanofabrication of cathode surfaces by reducing the emission area. We are inspired by nanotips used for electron microscopy where incident laser fields along with geometry-based field enhancement lead to electron emission via tunneling [1].

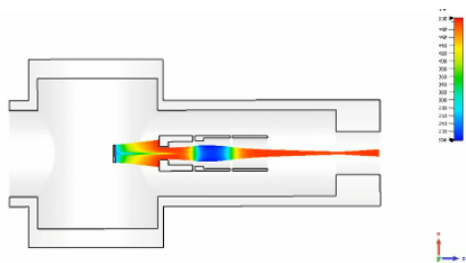


Figure 1: Cross section of vacuum chamber with electrostatic einzel lens and with example particle trajectories.

\* gelawler@physics.ucla.edu

Electron rescattering processes (denoted here by the cartoon schematic in Fig. 1) after emission increase the energy of the electrons notably. Tips work well but one major drawback is the damage they sustain at higher laser intensities. The current field limits are in the 10–20 GV/m range. Instead we opt for a more robust extended geometry which is shown in the micrograph in Fig. 2. The larger surface area allows for more robustness to laser illumination and can allow us to extract higher charge which is applicable to the needs of higher current accelerators. Our recipe and further explanation for the double blade geometry are historical and further information can be found in [2, 3]. We intend to quantify the intrinsic emittance from these nanoblades in order to continue to expand the space of possible applications these cathodes.

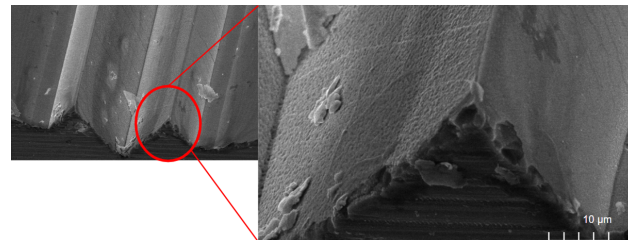


Figure 2: SEM image of nanoblades at ×5000 zoom.

## EXPERIMENT

### Einzel Lens

For simplification of the setup we can use a single einzel lens focusing our high aspect ratio beam on a multi-channel plate (MCP) and phosphor screen about 25 cm away from the cathode source. There does not exist a closed form solution of the focal length of a three element einzel lens but we can, for comparison, consider the limit where the lens distance is much greater than the aperture  $l \gg a$  and thus can obtain a usable expression.

$$\frac{1}{f} = \frac{3\kappa^2(4 - \kappa^2)}{8l(1 + \kappa)} \quad \text{where} \quad \kappa = \sqrt{\frac{V_1 + V_0}{V_0}} - 1 \quad (1)$$

With regards to the experimental setup, we illuminate our cathodes with an 800 nm, 35 fs pulse of the given peak intensities and spot size. Upstream of the blade sample location we have optics to control laser fluence, polarize the beam normal to the blade surface, and focus on the sample. Downstream we have a CCD camera for initial

sample alignment. We can see all of this in the schematic below. The vacuum chamber that houses the cathodes is depicted to the right. Emitted electrons here travel to the right, perpendicular to the laser path. The electrons pass through an einzel lens and are focused on an MCP detector about 29 cm away from the cathode location.

During emission measurements the sample is at a 0.5 degree angle such that it fully intercepts the 800 nm and most of the 15 mm long blade is illuminated. More information about the diagnostic setup can be found in [3].

## MEASUREMENTS

As a first measurement we can turn off the einzel lens and perform a biasing sweep of the cathode. We illuminate the cathodes at  $\approx 1$  degree to allow for full illumination of the blade. This, however, emits the electrons at a slight angle with respect to the longitudinal axis as shown in Fig. 1. We then expect a ramping of this bias to increase the signal up to a certain point at which the diverging electron beam will begin to miss the detector. We show this data in Fig. 3. We can then compare this data to curves calculated by assuming divergences corresponding to 0.01 eV up to 100 eV. By this coarse estimate we establish an initial upper bound of around 10 eV.

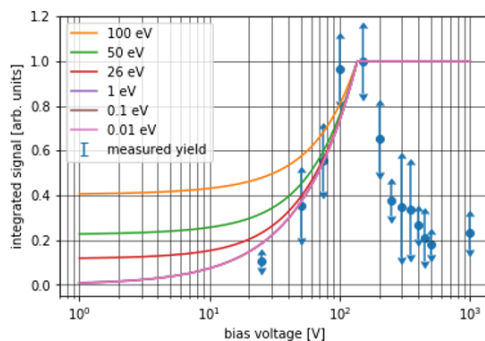


Figure 3: Electron signal in arb units as function of bias voltage on cathode. Note cathode at slight angle with respect to MCP in order to allow full illumination, hence the expected drop-off when the biased signal misses the detector.

The calculation here, however, is only for a point source so the results are only true in what we are calling the  $x$  direction which is in the direction of the blade spatial periodicity. By this we mean transverse to the blade ridge. We can then add a second blade as a second point source to this geometric analysis without significantly changing the results.

In the  $y$  direction, along the blade, this analysis is less accurate since the beams produced are an extended source. In order to make an assessment of the emittances here we initially attempted pinhole measurements, however the signal was too low. Instead we opted for an einzel lens scan with no collimation. In our measurements we observed effective beam waist-like structures for a number of different bias voltages each with interesting unexpected features. We classify these as waist-like rather than beam observations, the first

being that defocusing by overfocusing was not visible so no Rayleigh range was able to be measured. One such waist can is shown in data in Fig. 4.

Another notable feature was the presence of long extended line charge which curved around during focusing forming a lobe which eventually converges to form the minimum spot. We show what these lobes look like in the data in Fig. 5, showing the characteristic angle of the lobe structure. Note the intentional clipping on the left of the data in order to orient the focus.

## SIMULATION

We previously developed a beam dynamics workflow for simulating the experimental setup initially to optimize the lens geometry [2]. We can then use these simulations to track the high aspect ratio we are producing through the einzel lens setup and match the features observed in the data.

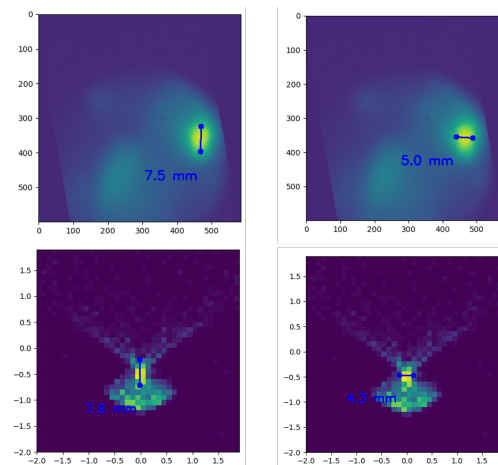


Figure 4: Comparison of beam “waists” experimentally measured to those reconstructed with simulation.

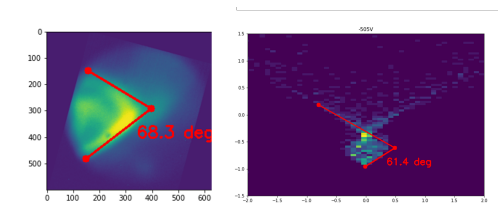


Figure 5: Comparison of beam lobe angle measurements and simulations.

## DISCUSSION

With our simulations, we identify most of the anomalous features with the high aspect ratio beams that are produced by the nanoblades. We note that the source size is approximately  $15 \text{ mm} \times 100 \mu\text{m}$  based on the full illumination of the blade. This is large compared to the aperture of the lens ( $\approx \text{cm}$  scale) which leads to significant nonlinear focusing. This

invalidates the simplified focal strength results contained in Eq. 1.

Instead, we find that the line charges combined with the slight nonzero angle of illumination leads to the lens focusing by looping the beam around, similar to a lasso. This forms the lobed structure and finally the effective beam waist followed by a quick disappearance on the phosphor screen rather than a similar defocus. We compare the simulations to data features in Figs. 4 and 5. We note that the size of the waists and angle of the lobed structure produced by the nonlinear focusing are well reproduced in simulation.

We can further use our simulations to establish a smaller lower bound on the mean transverse energy (MTE) by noting that feature preservation only occurs for an MTE less than 5 eV. We can see these simulations in Figs. 6 and 7. This value is in line with calculations and theory [4].

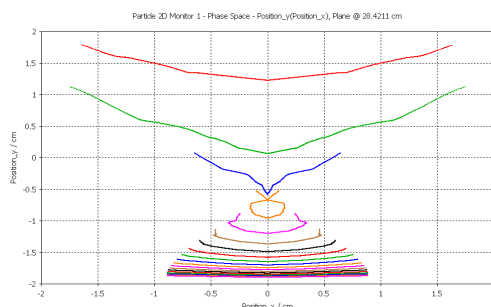


Figure 6: Reconstruction of transverse profile for monochromatic beams with 0 eV MTE.

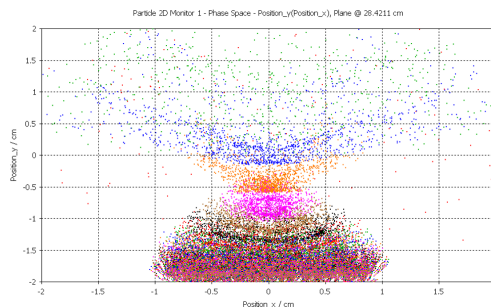


Figure 7: Reconstruction of transverse profile for monochromatic beams with 5 eV MTE.

### Emittance Reconstruction

We then take the simulations that accurately reproduce lens scan features and use them to establish an upper bound on the transverse emittances based on preservation of these features. We established these values to be  $\varepsilon_y = 42.6 \mu\text{m}$  rad;  $\varepsilon_x = 9.09 \mu\text{m}$  rad. Further emittance measurement precision in the short dimension is limited by the presence of the second blade. We also know from the implicit energy filtering of the einzel lens that electrons measured with energies in excess of 1 keV had energies of around 400-500 eV at emission.

### MC3: Novel Particle Sources and Acceleration Techniques

#### T02: Electron Sources

The transverse emittance in the  $x$  direction is within a reasonable number. However, we observe an unexpectedly higher emittance in the  $y$  direction. We attribute this to the presence of the secondary nanoblade. Historically, the second blade was fabricated for a number of reasons. The first was to make sure that the electron signal was high enough to observe. With these measurements we are now certain that we can halve the charge, by removing a nanoblade, and continue to perform reliable measurements. Going forward we can modify our recipe to not produce the second blade or we could consider removing one blade from the existing samples we have fabricated.

### CONCLUSIONS & FUTURE WORK

We have successfully produced a high aspect ratio high current beam from nanofabricated cathodes without long term damage. We have measured the upper bound on MTE and transverse emittance for novel nanofabricated cathodes. Seeing that our measurements are now limited by the presence of a second blade, we are motivated to remove one blade for future measurements. We show the result of and attempt to experiment with using focused ion beam (FIB) to remove one blade in Fig. 8.

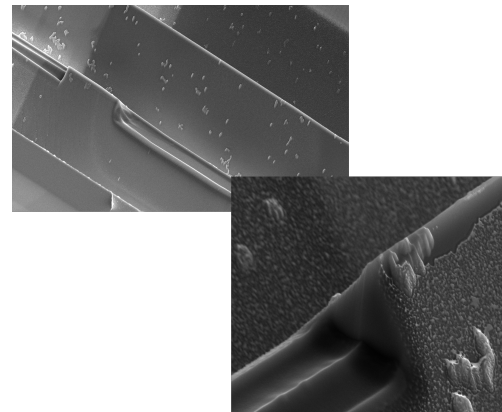


Figure 8: Experiment using focused ion beam (FIB) to remove one blade, simplifying the fabrication recipe.

We also have the possibility to use these structures as nanospray devices for vacuum propulsion of spacecraft. We are currently in collaboration with UCLA's engineering department in this regard.

### ACKNOWLEDGEMENTS

This work was supported by the Center for Bright Beams, National Science Foundation Grant No. PHY-1549132 and DOE HEP Grant DE-SC0009914.

### REFERENCES

- [1] M. Krüger, M. Schenk, P. Hommelhoff, G. Wachter, C. Lemell, and J. Burgdörfer, "Interaction of ultrashort laser pulses with metal nanotips: A model system for strong-field phenomena," *New Journal of Physics*, vol. 14, no. 8, p. 085019, 2012, doi: 10.1088/1367-2630/14/8/085019

- [2] G. Lawler, J. Mann, J. Rosenzweig, R. Roussel, and V. Yu, “Initial Nanoblade-Enhanced Laser-Induced Cathode Emission Measurements,” in *Proc. IPAC’21*, Campinas, SP, Brazil, 2021, paper WEPAB097, pp. 2814–2817.
- [3] G. Lawler *et al.*, “Electron diagnostics for extreme high brightness nano-blade field emission cathodes,” *Instruments*, vol. 3, no. 4, 2019, doi:10.3390/instruments3040057
- [4] J. Mann, T. Arias, G. Lawler, J. Nangoi, and J. Rosenzweig, “Simulations of Nanoblade-Enhanced Laser-Induced Cathode Emissions and Analyses of Yield, MTE, and Brightness,” in *Proc. IPAC’21*, Campinas, SP, Brazil, 2021, paper WEPAB147, pp. 2957–2960.